THE JOURNAL OF PHYSICAL CHEMISTRY A

Article

pubs.acs.org/JPCA

Why Is the L-Shaped Structure of $X_2\cdots X_2$ (X = F, Cl, Br, I) Complexes More Stable Than Other Structures?

Robert Sedlak,[†,§] Palanisamy Deepa,[†,§] and Pavel Hobza*[,†,‡]

[†]Institute of Organic Chemistry and Biochemistry, Academy of Sciences of the Czech Republic, Flemingovo nám. 2, 166 10 Prague 6, Czech Republic

[‡]Regional Centre of Advanced Technologies and Materials, Department of Physical Chemistry, Palacky University, 771 46 Olomouc, Czech Republic

Supporting Information

ABSTRACT: Five different structures (L- and T-shaped (LS, TS), parallel (P), parallel-displaced (PD), and linear (L)) of $(X_2)_2$ dimers (X = F, Cl, Br, I, N) have been investigated at B97-D3, M06-2X, DFT-SAPT, and CCSD(T) levels. The Q_{zz} component of the quadrupole moment of all dihalogens, which coincides with the main rotational axis of the symmetry of the molecule, has been shown to be positive, whereas that of dinitrogen is negative. All of these values correlate well with the most positive value of the electrostatic potential, which, for dihalogens, reflects the magnitude of the σ-hole. The LS structure is the most stable structure for all dihalogen dimers. This trend is the most pronounced in the case of iodine and bromine; for dinitrogen dimer, the LS, TS, and PD structures are comparably stable. The dominant stabilization energy for dihalogen dimers is dispersion energy, followed by Coulomb energy. In the case of dinitrogen dimer, it is only the dispersion energy. At short distances, the Coulomb (polarization) energy for dihalogen dimers is more attractive for the LS structure; at larger distances, the TS structure is more favorable, as dispersion and induction energies are systematically more stable for the TS structure. For all dimers and all distances, the long-range electrostatic energy covering the interactions of multipole moments is the most attractive for the TS structure. In the case of dihalogen dimers, the preference of the LS structure over the others, resulting from the concert action of Coulomb, dispersion, and induction energies, is explained by the presence of a σ-hole. In the case of dinitrogen, comparable stability of LS, TS, and PD structures is obtained, as all are dominantly stabilized by dispersion energy.

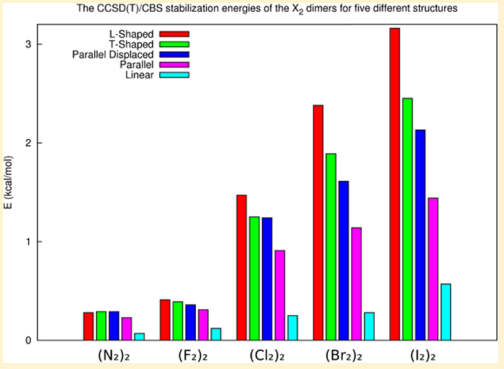

INTRODUCTION

The first nonzero electric multipole moment of dihalogens (X_2, X = F, Cl, Br, I) is the quadrupole moment (Q_{zz}), which is positive for all of these systems. In a simplified notation, these quadrupole moments may be written as + − − +. The quadrupole moment of other diatomics such as dinitrogen is negative and the simplified notation is − + + −. The explanation of the different signs of quadrupole moments of the dihalogens and dinitrogen is not easy because both halogens and nitrogen bear lone electron pairs and pair, respectively. This is in accord with the sign of the quadrupole moment of dinitrogen but not with that of dihalogens.[1,2] To our knowledge, no easy explanation of this fact was available until the recent introduction of the σ-hole, which has been used to explain the origin of the attraction in the halogen bond.[3]

The existence of halogen bonding, described as an attractive interaction between a bound halogen and an electronegative atom, seems counterintuitive, given that an attractive noncovalent interaction is not expected to exist between two atoms that have high electronegativity, that is, possess a partial negative charge. The reason for the attractive noncovalent interaction that occurs in halogen bonds is the presence of a region of a positive electrostatic potential (σ-hole) along the extension of the C−X bond (X is most typically bound to carbon), which interacts electrostatically with an electron donor.[4,5] Here, we present the recent IUPAC definition of the halogen bonding: "A halogen bond occurs when there is evidence of a net attractive interaction between an electrophilic region associated with a halogen atom in a molecular entity and a nucleophilic region in another, or the same, molecular entity."[6,7]

The existence of the positive σ-hole explains positive quadrupole moments in dihalogens; similarly, the nonexistence of the σ-hole in dinitrogen explains its negative quadrupole moment. Are the two concepts fully equivalent? In other words, do they both lead to the same structure prediction? Certainly, such a comparison is limited to systems where the first nonvanishing multipole moment is the quadrupole moment. In other cases (i.e. for systems with dipole moments), the concept of the σ-hole is clearly the only applicable explanation. We

Received: March 17, 2014
Revised: May 5, 2014
Published: May 5, 2014

   dx.doi.org/10.1021/jp502648e | J. Phys. Chem. A 2014, 118, 3846−3855

should mention a study done by Duarte et al.,[8] in which analyses of atomic quadrupole moments of halogens were performed for halogen bonded complexes.

The aim of the present paper is to investigate different structures of the (X_2, X = F, Cl, Br, I, N) complexes.

CALCULATIONS

The electrostatic potential (ESP)[9−12] computed for all subsystems at the B97/def2-QZVP,[13,14] HF/aug-cc-pVTZ,[15−19] PBE0/aug-cc-pVTZ,[20−22] MP2/aug-cc-pVTZ,[23] and CISD/aug-cc-pVTZ[24] levels was determined on the 0.001 au (e^-/Bohr^3) isodensity surface, as proposed by Bader et al.[25] The point on the 0.001 au isodensity surface, which lies on the main rotational axis of the X_2 molecule, is referred to here as $V_{s,max}$ (Figures S1 and S2, Supporting Information). In the case of dihalogens, this point possesses the most positive value of the ESP (the local maximum). The angular dependence of the ESP was also investigated. The angle α, at which the ESP becomes negative when moving from the $V_{s,max}$ point on the 0.001 isodensity surface, was evaluated. The $V_{s,max}$ and α quantities are the magnitude and the size of the σ-hole and have been defined by Kolář et al.[26] For more details concerning $V_{s,max}$ and α, see the Supporting Information or ref 26.

The benchmark stabilization energies were obtained from CCSD(T)/CBS calculations. The DFT-SAPT method has been shown to provide a reliable estimation of the stabilization energies of various noncovalent interactions including the halogen bond.[27−38] Hence, the DFT-SAPT calculations were used for the decomposition of the total interaction energy.

The relativistic effects were included by considering the pseudopotentials (PPs).[39,40] Specifically, for bromine and iodine at the HF, PBE0, MP2, CCSD(T)/CBS, DFT-SAPT, and CISD levels, PPs consistent with respective correlation consistent basis sets (aug-cc-pVXZ-PP) were applied. At the B97-D3/def2-QZVP level, the PPs were considered only for iodine.

Five different structures of the $(X_2)_2$ dimers (L-shaped (LS), T-shaped (TS), parallel (P), parallel-displaced (PD), and linear (L)) were considered, and the respective energy minima were determined by an unrelaxed potential energy scan along the main intermolecular coordinates (Figure 1). The scans were performed on the grid with a point-to-point distance of 0.1 Å. The geometries of the X_2 molecules considered for all calculations were calculated at the B97-D3/def2-QZVP level of theory.

The benchmark interaction energies were evaluated at the CCSD(T) level and extrapolated to the complete basis set (CBS) limit. Specifically, the CCSD(T)/CBS interaction energy was constructed as the sum of HF/CBS interaction energy and the correlation part of the MP2/CBS interaction energy. Both were determined by the two-point extrapolation scheme of Halkier from aug-cc-pVTZ and aug-cc-pVQZ basis sets.[41,42] The CCSD(T) correction term ($\Delta E^{CCSD(T)} - \Delta E^{MP2}$) was evaluated utilizing the aug-cc-pVTZ basis set.[43−46] Besides CCSD(T), two variants of the DFT method were applied. The M06-2X functional[47] was recommended for calculations of halogen-bonded complexes.[48] Therefore, this functional in combination with the aug-cc-pVTZ basis set was used in the present study along with the DFT-D (B97-D3/def2-QZVP) method.[49] The Grimme's empirical dispersion correction (D3) was calculated employing Becke−Johnson damping.[50]

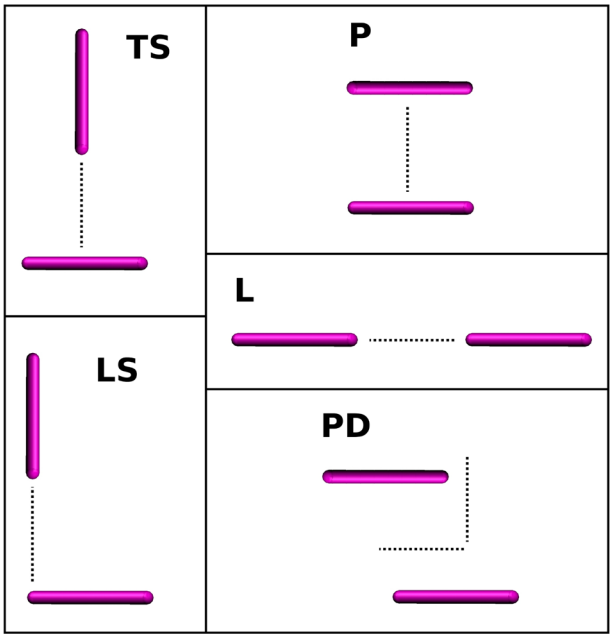

Figure 1. The five conformers that were considered for each homodimer. The intermolecular coordinate along which the unrelaxed scan was performed is also depicted. LS, TS, P, PD, and L stand for L-shaped, T-shaped, parallel, parallel-displaced, and linear, respectively.

The decomposition of stabilization energy was obtained by using the SAPT method,[51] specifically the DFT-SAPT technique. The subsystems were treated via the DFT approach, utilizing the asymptotically corrected LPBE0AC exchange-correlation functional[52,57] and the aug-cc-pVTZ basis set for nitrogen, fluorine, and chlorine. In the case of bromine and iodine, the aug-cc-pVTZ-PP basis set was used to account for relativistic effects.[39,40] The DFT-SAPT total interaction energy is given as the sum of the first- (E_1) and second-order (E_2) perturbation energy terms and δHF energy terms, specifically Coulomb (E_1^{Pol}), induction (E_2^{I}), and dispersion (E_2^{D}), together with exchange-repulsion terms (E_1^{Ex}, $E_2^{Ex\text{-}I}$, $E_2^{Ex\text{-}D}$). The exchange-induction and exchange-dispersion terms are merged into the respective induction and dispersion terms. Further, the δHF term, which represents higher than second-order terms covered by the Hartree−Fock approach, is also included in the induction energy.

$$E_{int} = E_1^{Pol} + E_1^{Ex} + E_2^{I} + E_2^{Ex\text{-}I} + \delta HF + E_2^{D} + E_2^{Ex\text{-}D} = E_1^{Pol} + E_1^{Ex} + E_2^{Ind} + E_2^{Disp} \quad (1)$$

More details about the DFT-SAPT calculations can be found in refs 53−59.

Finally, the long-range electrostatic interaction energy between two subsystems covering interactions of multipoles was calculated using the distributed multipole analysis of Stone.[60−62] The multipole moments were calculated on the basis of the PBE0/aug-cc-pVTZ wave function using the GDMA program.[63] Subsequently, the electrostatic interactions between molecules were calculated via the Orient program.[64] The diatomic molecule was represented by three sites. Two of these sites coincide with X atoms, and the third one was located in the middle of the X−X bond. Each site was constituted by the multipole moments up to the hexadecupole. For the technical details of the distributed multipole moment analysis, see ref 62.

dx.doi.org/10.1021/jp502648e | J. Phys. Chem. A 2014, 118, 3846−3855

All of the post Hartree−Fock calculations (MP2, CCSD(T), and DFT-SAPT) were carried out using the MOLPRO 2010 software package.[65] The convergence threshold imposed on the change in energy and root-mean-square deviation (RMSD) of the density matrix between consecutive SCF iterations was set to 10^{-9} and 10^{-6} au, respectively. The CCSD convergence criteria were set to 10^{-8} au for the energy change and 10^{-8} au for the square sum of the changes of the CC amplitudes. The DFT-based methods, excluding M06-2X, were applied utilizing the TURBOMOLE 6.3 software package.[66] The TURBOMOLE grid m3 was consistently used for integral evaluation in all the calculations. The convergence criteria were set to 10^{-7} and 10^{-6} au for the energy change and RMSD of the density matrix, respectively. The M06-2X and population analysis[67] calculations were carried out using the Gaussian 09 software package,[68] employing default convergence criteria and a default fine grid for integral evaluation. All of the interaction energy calculations were corrected for the basis set superposition error employing counterpoise correction.[69] A full description of the material can be found in the Supporting Information.

RESULTS AND DISCUSSION

Isolated Systems. Table 1 summarizes the geometries, quadrupole moments, and size (α) and magnitude ($V_{s,max}$)[26] of

Table 1. Geometries, Quadrupole Moments, and $V_{s,max}$ for all Monomers Calculated at the B97/def2-QZVP Level of Theory

systems	geometries (Å)	quadruple moment[a]	$V_{s,max}$ (au)[b]
I_2	2.703	3.402	0.0474
Br_2	2.322	2.362	0.0443
Cl_2	2.013	1.574	0.0389
F_2	1.410	0.436	0.0243
N_2	1.116	−0.774	−0.0140

[a]The Q_{zz} component in ea_o^2. [b]Calculated at the 0.001 au isodensity surface.

σ-holes calculated for all subsystems at the B97/def2-QZVP level of theory. The electrostatic potential for all subsystems is visualized in Figure 2. Clearly, the quadrupole moments of all dihalogens are positive, while the quadrupole moment of dinitrogen is negative. The same is valid for the magnitudes of the σ-holes ($V_{s,max}$). The negative value of $V_{s,max}$ for dinitrogen

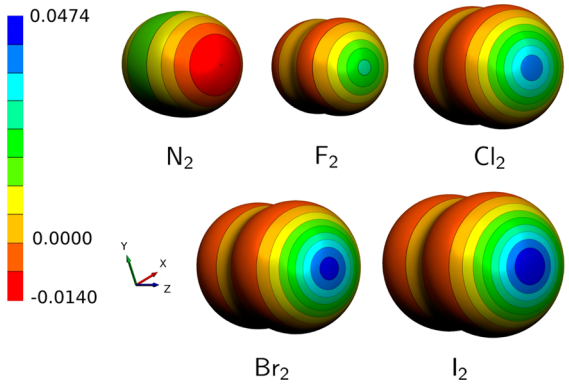

Figure 2. Electrostatic potential (in au) mapped on the 0.001 au isodensity surface for all monomers calculated at the B97/def2-QZVP level of theory. The z axis coincides with the main rotational axis of the molecule (the X−X bond direction).

indicates that the positive σ-hole is not present. The largest absolute value of both characteristics (quadrupole moments and $V_{s,max}$) was found for diiodine, and the smallest positive one was found for difluorine (the smallest $V_{s,max}$ was calculated for dinitrogen); quadrupole moments and $V_{s,max}$ correlate very well (R^2 = 0.849) for all systems.

This finding is important because it shows that at least for the systems studied (and similar systems for which the first nonzero multipole moment is quadrupole) their nontrivial electronic structure is described already by the classical concept of electric quadrupoles and that the recently introduced new concept of the σ-hole is not bringing any new information.

Table S1 (Supporting Information) compares the quadrupole moments (Q_{zz}) calculated at the B97/def2-QZVP, PBE0/aug-cc-pVTZ, HF/aug-cc-pVTZ, MP2/aug-cc-pVTZ, and CISD/aug-cc-pVTZ (as reference) levels of theory. We have done these calculations to verify the reliability of the DFT methods in providing accurate electrostatic properties because our further discussions are based on DFT calculations. The DFT and MP2 methods provide reliable values of quadrupole moments for all the molecules with respect to the reference CISD data (Table S1, Supporting Information). The only exception is the large underestimation of the quadrupole moment at the HF level for the F_2 molecule. This failure of the HF method to provide an accurate quadrupole moment for the F_2 molecule has already been discussed in the literature, see ref 1 and the references therein. It is attributed to the extremely compact character of the valence orbitals of the F_2 molecule.[1] However, in the case of the DFT (PBE0, B97) methods, no such discrepancy has been observed for this anomalous molecule. This is encouraging and serves as a proof that the use of the DFT methods for these purposes is legitimate.

Table S2 (Supporting Information) materials lists $V_{s,max}$ and the qaudrupole-moment (Q_{zz}) values for all diatomics at all the levels of theory mentioned. The high correlation between these two quantities can be observed for all of the methods tested. The correlation coefficient (R^2) amounts to 0.838, 0.849, 0.852, 0.858, and 0.869 for MP2, B97, CISD, PBE0, and HF, respectively. These results only support the already stated conclusion about the close relation between Q_{zz} and $V_{s,max}$.

Table 2 presents the X−X bond orbital analysis together with the occupancy of the p-type valence natural atomic orbitals (NAOs) and $V_{s,max}$ values. It further lists the size (angle α) and magnitude ($V_{s,max}$) of the σ-hole. The angle α varies between 59° (F_2) and 65°(I_2). When one moves from difluorine toward heavier dihalogens, the slight increase of α is in correlation with the significant increase of $V_{s,max}$. The small variation of the size of the σ-hole can be interpreted using the natural-bond orbital (NBO) analysis.[67]

First, the hybridization between s and p orbitals, in the case of the X−X natural-bond orbital, is negligible, not exceeding 6% (dichlorine). Second, the occupancy of p-type valence NAOs does not differ much between different halogens. Specifically, the valence p_z occupancy varies between 1.022 (I_2) and 1.043 (Cl_2). Moreover, the occupancy of the p_x and p_z orbitals is essentially constant. Finally, it is clear that the hybridization state and the occupancy of NAO are more or less constant for all dihalogens. Consequently, we conclude that the angular redistribution of the valence electrons is very similar for all dihalogens. Hence, marginal differences in the size of the σ-hole are observed. On the other hand, the possible explanation for the relatively large increase of the $V_{s,max}$ value (Table 1) can be seen as a consequence of the decreasing ability of the electron

Table 2. Hybridization State (%) of the Natural Hybrid Orbital (NHO) of Atom X in the Natural X−X Bonding Orbital, Occupancies of the p-Type Valence Natural Atomic Orbitals of Atom X, $V_{s,max}$, and the Size of the σ-hole (α)[a]

	NHOs of X−X NBOs					NAOs of p-type valence				
X	s	p	d	f	g	p_x	p_y	p_z[b]	$V_{s,max}$ (au)[c]	α (deg)[c]
F	4.9	94.9	0.2	0.1	0.0	1.999	1.999	1.038	0.0243	59
Cl	6.2	92.5	1.0	0.3	0.0	1.992	1.992	1.043	0.0389	62
Br	4.3	94.8	0.6	0.2	0.0	1.994	1.994	1.029	0.0443	64
I	3.5	95.6	0.5	0.3	0.0	1.994	1.994	1.022	0.0474	65
N	36.6[d]	62.9[d]	0.5[d]	0.0[d]	0.0[d]	0.996	0.996	1.325	−0.0140	
	0.0[e]	99.6[e]	0.4[e]	0.0[e]	0.0[e]					

[a]All data correspond to the B97/def2-QZVP densities and B97-D3/def2-QZVP geometries of X_2 molecules. [b]The z axis coincides with the X−X bond. [c]Calculated at the 0.001 au isodensity surface. For more details, see the Supporting Information. [d]The numbers correspond to s-type NBOs. [e]The numbers correspond to p-type NBOs.

Table 3. Interaction Energies (kcal/mol) Calculated at the B97-D3, M062X, CCSD(T)/CBS, and DFT-SAPT Levels of Theory for L-Shaped (LS), T-Shaped (TS), Parallel (P), Parallel-Displaced (PD), and Linear (L) Structures[a]

		R/R'	B97-D3	R/R'	M06-2X	R/R'	CCSD(T)/CBS	DFT-SAPT
LS	I_2	3.5/5.0	−4.77 (−3.44)	3.6/5.1	−2.96	3.6/5.1	−3.16	−3.64
	Br_2	3.3/4.6	−2.86 (−2.68)	3.3/4.6	−2.31	3.4/4.7	−2.38	−2.47
	Cl_2	3.3/4.4	−1.58 (−1.94)	3.2/4.3	−1.18	3.3/4.4	−1.47	−1.20
	F_2	3.2/4.0	−0.30 (−0.23)	2.9/3.7	−0.39	2.8/3.6	−0.41	−0.30
	N_2	3.7/4.3	−0.47 (−0.46)	3.8/4.4	−0.21	3.6/4.2	−0.28	−0.26
TS	I_2	4.1/5.2	−3.04 (−3.23)	4.0/5.1	−2.27	4.1/5.2	−2.45	−2.61
	Br_2	3.9/4.9	−1.96 (−2.25)	3.7/4.7	−1.61	3.7/4.7	−1.89	−1.93
	Cl_2	3.7/4.6	−1.25 (−1.69)	3.5/4.4	−0.87	3.6/4.5	−1.25	−1.05
	F_2	3.2/3.8	−0.29 (−0.24)	3.0/3.6	−0.38	3.0/3.6	−0.39	−0.31
	N_2	3.7/4.2	−0.48 (−0.45)	3.8/4.3	−0.21	3.6/4.1	−0.29	−0.27
P	I_2	4.5/4.5	−2.22 (−3.36)	4.4/4.4	−0.53	4.5/4.5	−1.44	−1.46
	Br_2	4.2/4.2	−1.50 (−2.39)	4.2/4.2	−0.37	4.2/4.2	−1.14	−1.08
	Cl_2	4.1/4.1	−1.04 (−1.49)	4.0/4.0	−0.40	3.9/3.9	−0.91	−0.78
	F_2	3.6/3.6	−0.26 (−0.22)	3.1/3.1	−0.36	3.2/3.2	−0.31	−0.25
	N_2	3.8/3.8	−0.51 (−0.57)	4.0/4.0	−0.20	3.7/3.7	−0.23	−0.22
PD	I_2	4.5/4.5	−2.82 (−3.85)	4.3/4.3	−1.73	4.4/4.4	−2.13	−2.26
	Br_2	4.2/4.2	−1.83 (−2.64)	4.0/4.0	−1.19	4.0/4.0	−1.61	−1.58
	Cl_2	3.9/3.9	−1.23 (−2.08)	3.7/3.7	−0.89	3.8/3.8	−1.24	−1.02
	F_2	3.6/3.6	−0.26 (−0.25)	3.3/3.3	−0.34	3.2/3.2	−0.36	−0.28
	N_2	3.9/3.9	−0.55 (−0.60)	4.4/4.4	−0.20	4.0/4.0	−0.31	−0.29
L	I_2	4.2/6.9	−0.72 (−1.61)	3.8/6.5	−0.18	3.9/6.6	−0.57	−0.44
	Br_2	4.1/6.4	−0.43 (−1.01)	3.5/5.8	0.17	3.7/6.0	−0.28	−0.15
	Cl_2	3.8/5.8	−0.34 (−0.81)	4.1/6.1	0.02	3.5/5.5	−0.25	−0.11
	F_2	3.3/4.7	−0.11 (−0.13)	3.0/4.4	−0.14	2.9/4.3	−0.12	−0.11
	N_2	3.9/5.0	−0.13 (−0.20)	4.0/5.1	−0.09	3.7/4.8	−0.07	−0.07

[a]The numbers in parentheses correspond to dispersion energy. R and R' correspond to the closest X···X and center of mass distances (in Å), respectively.

shell to shield the nucleus. In other words, the shielding of the nucleus charge is more significant in the case of the compact electron shell (e.g., fluorine, chlorine) than in the case of the diffuse one (e.g., bromine, iodine).

The character of the electron redistribution is entirely different for the dinitrogen molecule when compared with dihalogens. The triple bond is represented by two π- and one σ-bond orbitals within the NBO analysis (Table 2).

The sign of the $V_{s,max}$ value, which is positive in the case of dihalogens and negative for dinitrogen, can be interpreted by means of the relative occupancy of the NAOs of the valence p type.[2] In the case of dihalogens, the lack of electron density is observed in the z axis, which coincides with the X−X bond when compared with the x and y axes. In the case of dinitrogen, the opposite is true (Table 2).

Complexes. The total interaction energies of all dihalogen dimers determined by the B97-D3, M06-2X, CCSD(T), and DFT-SAPT techniques are given in Table 3. The numbers in parentheses listed with the B97-D3 energies correspond to the respective empirical dispersion energies. In the case of DFT-SAPT calculations presented in Table 3, the potential-energy scans were not made, and the values correspond to the structures, which represent the CCSD(T)/CBS energy minima.

Stabilization energies evaluated at different levels of theory correlate well with reference CCSD(T) stabilization energies. Specifically, correlation coefficient (R^2) amounts to 0.95, 0.92, and 0.99 for the B97-D3, M06-2X, and DFT-SAPT method. The general performance of listed methods, which can be judged on the basis of the value of the root-mean-square deviation (RMSD) with respect to reference data, is following. The most accurate method is DFT-SAPT followed by M06-2X

dx.doi.org/10.1021/jp502648e | J. Phys. Chem. A 2014, 118, 3846−3855

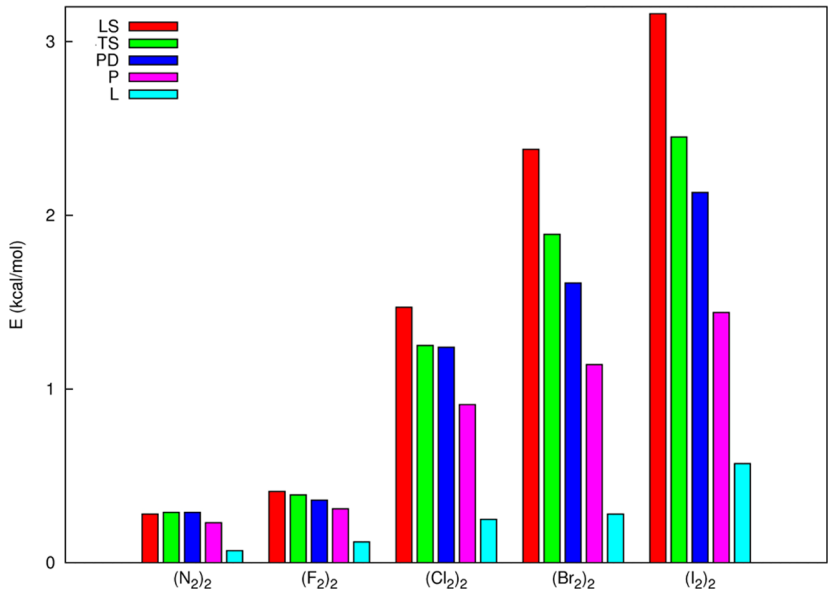

Figure 3. CCSD(T)/CBS stabilization energies (in kcal/mol) for all complexes. LS, TS, P, PD, and L stand for L-shaped, T-shaped, parallel, parallel-displaced, and linear, respectively.

and B97-D3. Corresponding RMSD values are 0.15, 0.34, and 0.44 kcal/mol.

Specifically, the B97-D3 interaction energies are mostly the largest ones and are, especially for the heavier dihalogens, strongly overestimated (with respect to the CCSD(T)/CBS benchmark values). The average absolute (relative) errors for chlorine, bromine, and iodine are −0.06 (11), −0.26 (25), and −0.76 kcal/mol (38%), respectively. The same feature of overestimation is observed for nitrogen. Error amounts to −0.19 kcal/mol (85%). However, in the case of fluorine, the interaction energies are underestimated. The average absolute (relative) error is 0.07 kcal/mol (−21%).

The M06-2X method exhibits opposite trends. In the case of fluorine, the interaction energies are overestimated. The absolute (average) error is −0.03 kcal/mol (12%), whereas the average absolute (relative) errors for chlorine, bromine, iodine, and nitrogen are 0.34 (−47), 0.38 (−53), 0.42 (−33), and 0.05 kcal/mol (−13%), respectively.

DFT-SAPT energies match closely with the benchmark data. The relatively low overestimation for iodine complexes is −0.13 kcal/mol (1%). The underestimation is observed for the rest of the complexes and varies from 0.01 kcal/mol (−5%) for nitrogen up to 0.19 kcal/mol (−25%) for chlorine.

Investigating the reference CCSD(T)/CBS stabilization energies of dihalogen complexes, we found that the LS structure corresponds with the most stable structure (i.e., the global minimum), followed by the TS, PD, P, and L structures. For heavier dihalogens, the LS and TS structures are more stable than other structures; in the case of difluorine, all the structures, except linear (L), are comparably stable (Figure 3). This finding is surprising because it was long believed that the TS structure of dihalogens, stabilized by quadrupole−quadrupole electrostatic interaction, corresponds to the global minimum. Moreover, Table 3 (the last column labeled as R/R') shows that the intermolecular distances between the centers of mass for the optimized LS and TS structures are similar.

The DFT-SAPT total interaction energies of all dihalogen dimers are the most negative for the LS structure (Table 3). Analyzing the DFT-SAPT energy components (Figure 4), we found that this is mainly caused by the Coulomb E_1^{Pol} energies. The other attractive energies (dispersion and induction) are also the largest for the LS structure, but the absolute difference with respect to other structures (TS, PD, P, and L) is much smaller. This can be interpreted as a consequence of the higher orientation dependence of the Coulomb interaction, in contrast with induction and dispersion. However, it should be stressed that the largest attractive contribution for all structures (including LS and TS) comes from dispersion energy, followed by Coulomb energy.

To exclude the overlap effects (see below), we evaluate the total interaction energies at the DFT-SAPT level for the two most stable structures (LS and TS) and for larger intermolecular distances. These scans are performed for the diiodine dimer and will be discussed in the following paragraphs. Figure 5 shows the distance dependence of the total DFT-SAPT as well as Coulomb (E_1^{Pol}) energies for the LS and TS structures of the diiodine dimer. At short distances, the Coulomb energy is evidently more attractive for the LS structure, while the opposite is true at larger distances. On the other hand, the total DFT-SAPT energy is systematically larger for the LS structure. This finding can be easily explained on the basis of penetration energy.[51] The systematically attractive penetration energy, which is included in the DFT-SAPT Coulomb energy, is overlap-dependent. The overlap in the LS structure is clearly larger than that in the TS structure because of a closer X···X contact in the former structure. At large distances, the penetration of both molecules becomes negligible and the DFT-SAPT Coulomb energy is exclusively represented by long-range electrostatic energy. The long-range electrostatic energy covering all the interactions between the multipole moments is less attractive for the L-shaped structure than for the T-shaped structure (Figure 6).

We should summarize the previous findings. In the whole range of distances, the stabilization energy of the LS structure is larger than that of the TS structure, while the opposite is true for the long-range electrostatic energy. The Coulomb energy is larger for the LS structure only at short distances. The question

dx.doi.org/10.1021/jp502648e | J. Phys. Chem. A 2014, 118, 3846−3855

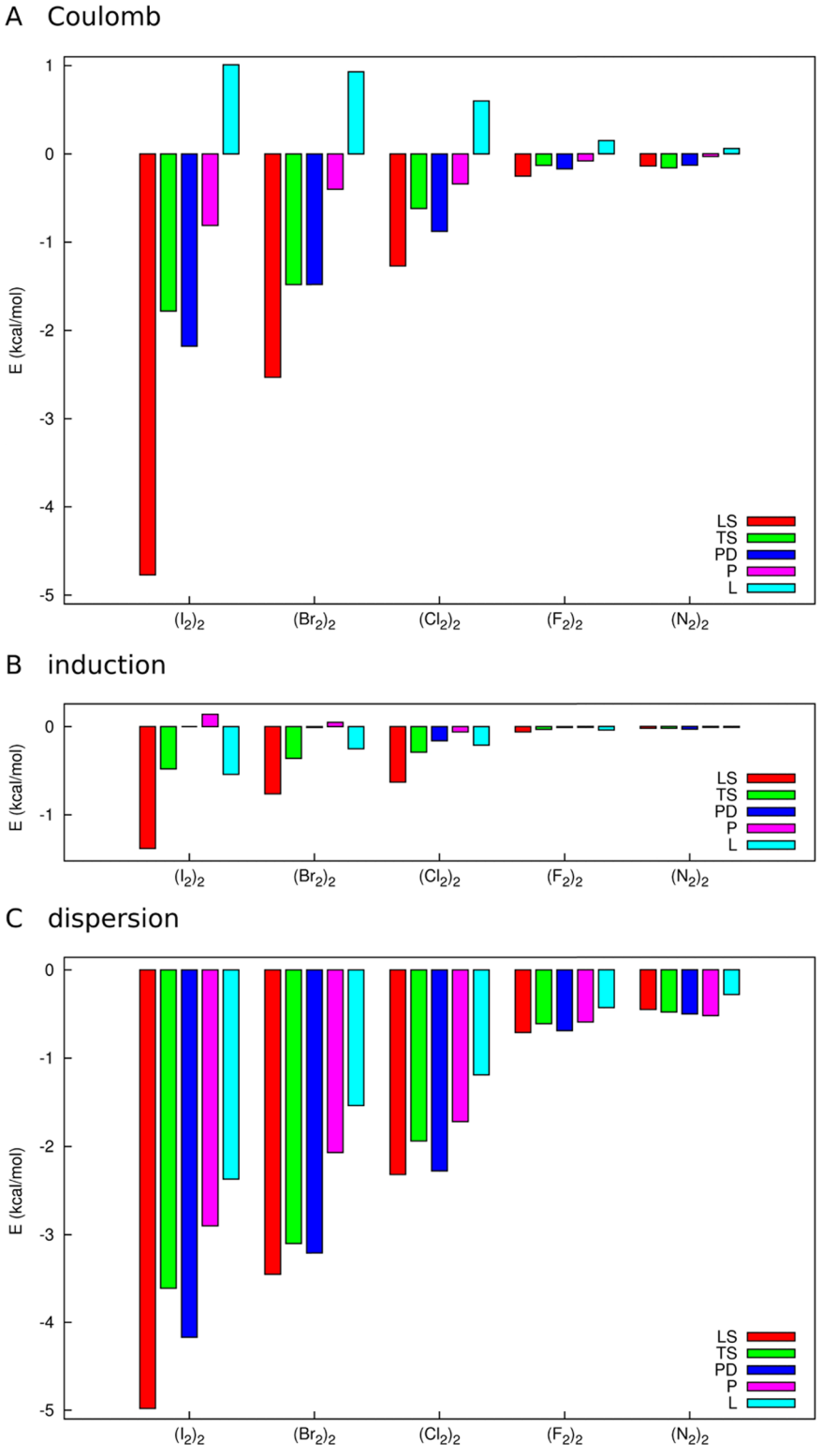

Figure 4. Coulomb E_1^{Pol} (A), induction E_2^{Ind} (B), and dispersion E_2^{Disp} (C) components of the DFT-SAPT interaction energy (in kcal/mol), listed for all five structures of each complex. For exact definitions of Coulomb, induction, and dispersion, see the Calculations section.

is how to explain the larger stabilization energy in the L-shaped structure. Figure 7 shows the distance dependence of the remaining attractive energy terms, dispersion (E_2^{Disp}) and induction (E_2^{Ind}). It is evident that both energies are systematically more attractive for the LS structure. This was also observed for equilibrium geometries (see above). The reason for this is again the shorter interatomic distances for the LS structure. The preference of the LS structure in the entire distance region cannot be explained by either electrostatic or Coulomb energies. It is a result of the concert action of all three attractive energies, Coulomb, dispersion and induction.

The interaction interpreted via quadrupoles prefers the T-shaped structure, but the full QM treatment leads to the L-shaped structure. An alternative description of the monomers is

dx.doi.org/10.1021/jp502648e | J. Phys. Chem. A 2014, 118, 3846−3855

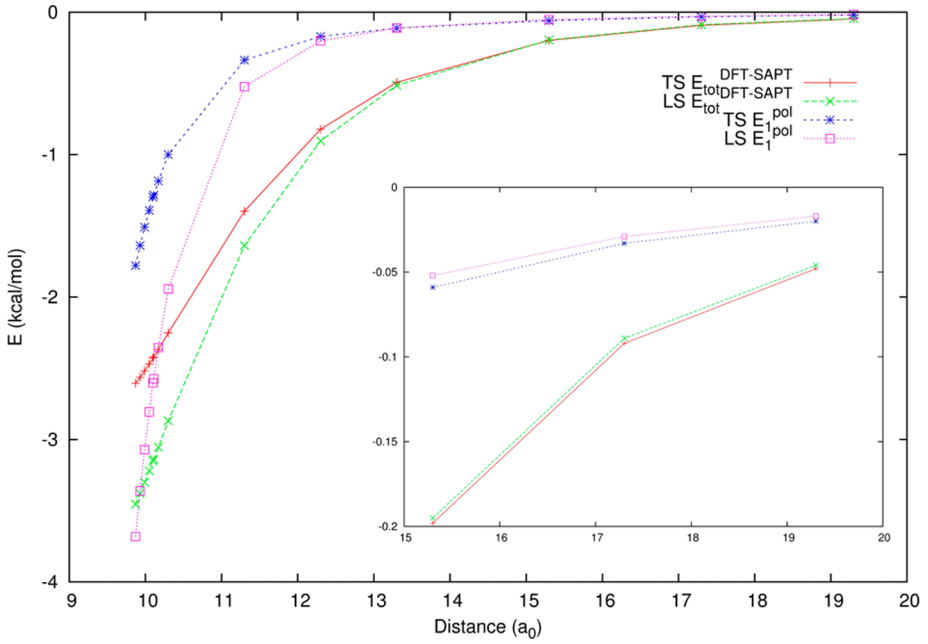

Figure 5. Distance dependence of the total interaction ($E_{tot}^{DFT\text{-}SAPT}$) and Coulomb ($E_1^{Pol}$) energies for LS and TS structures of the diiodine dimer calculated at DFT-SAPT/aug-cc-pVTZ-PP level of theory. All energies are listed in kilocalories per mole (kcal/mol).

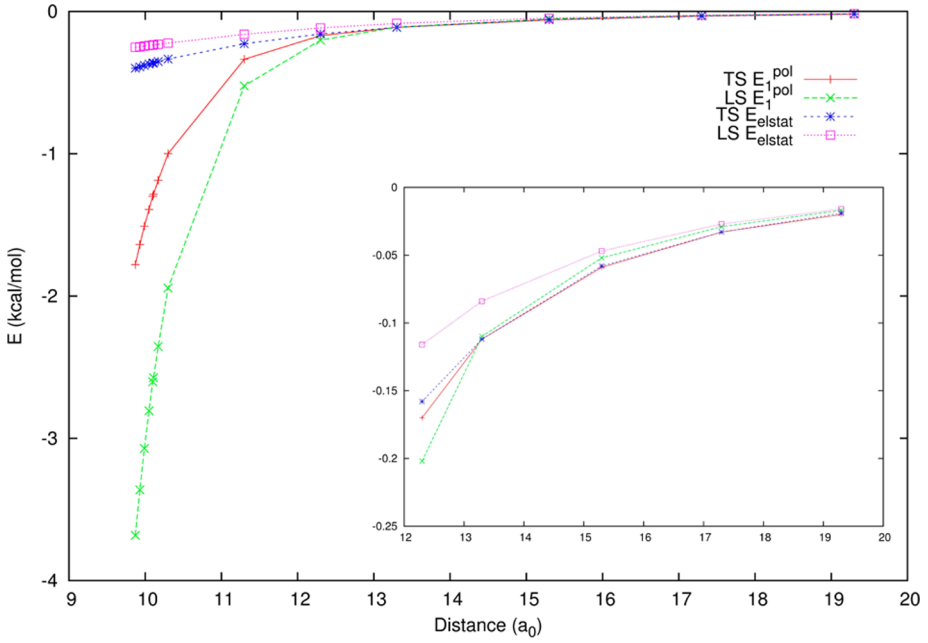

Figure 6. Distance dependence of electrostatic (E_{elstat}) and Coulomb (E_1^{Pol}) energies for the LS and TS structures of the diiodine dimer calculated using distributed multipole analysis[57−59] and the DFT-SAPT/aug-cc-pVTZ-PP level of theory, respectively. All energies are listed in kilocalories per mole (kcal/mol).

provided by the concept of electrostatic potential, for example, the σ-hole (see above). The question arises whether the interaction of two dihalogens, each possessing the σ-hole, can be explained or at least schematically interpreted on the basis of the monomer electrostatic potential. Another question is whether it would be possible to explain the preferential binding of the L-shaped structure within this concept. Figure 8 schematically shows the LS and TS structures together with the ESP of isolated molecules. Evidently, the first structure exhibits a strong attractive electrostatic interaction between the most positive σ-hole of the upper (vertical) dihalogen and the less positive belt of the lower (horizontal) one (the so-called dihalogen bond). Such an interaction is not expressed as strongly in the T-shaped structure. Thus, it is possible to conclude that the preferential binding of the LS structure in all the dihalogen dimers investigated can be interpreted by the dihalogen bonding. The classical concept of electric multipoles cannot be used because it leads to preferential binding in the TS structure.

The situation with dinitrogen not possessing the σ-hole is different. Here, the total stabilization energy at the CCSD(T)/CBS level is comparable for the LS, TS, and PD structures. The

dx.doi.org/10.1021/jp502648e | J. Phys. Chem. A 2014, 118, 3846−3855

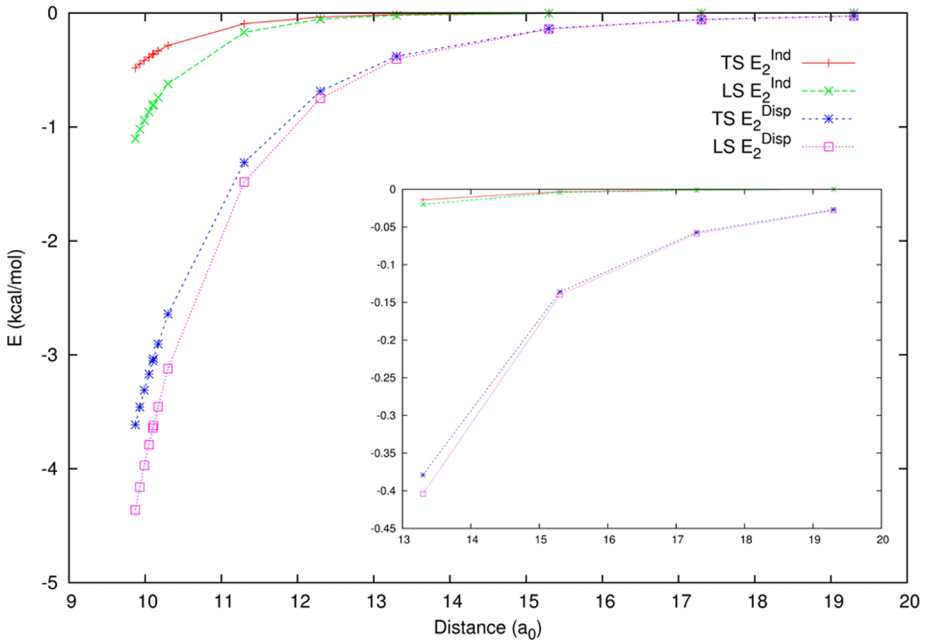

Figure 7. Distance dependence of induction (E_2^{Ind}) and dispersion (E_2^{Disp}) energies for the LS and TS structures of the diiodine dimer calculated at the DFT-SAPT/aug-cc-pVTZ-PP level of theory. All energies are listed in kilocalories per mole (kcal/mol).

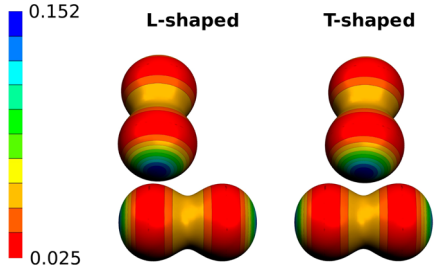

Figure 8. L-shaped (left) and T-shaped (right) structures of the X_2 dimer. A schematic interpretation of the electrostatic interaction based on the electrostatic potentials (ESP, in au) of isolated monomers. The ESP is mapped on the 0.01 au isodensity surface to prevent the overlap of the electron densities.

L and P structures are less stable (Figure 3). Analyzing the DFT-SAPT energies, we found that dispersion energy is clearly a dominant stabilization term for all five conformers (Figure 4), while Coulomb energy is marginal. It could thus be concluded that the preference of the LS structure found in dihalogen dimers arises from the presence of the σ-hole, or, in other words, the presence of the dihalogen bond. In this case, Coulomb energy is important. On the other hand, when the σ-hole is absent, Coulomb energy is negligible, and dispersion energy becomes clearly dominant.

CONCLUSIONS

The most stable structure among the complexes of homodiatomics possessing the σ-hole is the LS structure. For dinitrogen dimer (a system without the σ-hole), it is TS structure. The stabilization in the former case results from the existence of a dihalogen bond having comparable Coulomb and dispersion energies. The TS structure of dinitrogen dimer is stabilized dominantly by dispersion energy.

ASSOCIATED CONTENT

Supporting Information

Schematic representation of the grid orientation of the X_2 molecule; definition of the σ-hole size; and $V_{s,max}$ (in au) and quadrupole moment (Q_{zz} in au) values for all diatomics (F_2, Cl_2, Br_2, I_2 and N_2). This material is available free of charge via the Internet at http://pubs.acs.org.

AUTHOR INFORMATION

Corresponding Author

*E-mail: pavel.hobza@uochb.cas.cz.

Author Contributions

§Both authors have contributed equally and can be considered as the first author.

Notes

The authors declare no competing financial interest.

ACKNOWLEDGMENTS

This work was part of the Research Project RVO: 61388963 of the Institute of Organic Chemistry and Biochemistry, Academy of Sciences of the Czech Republic. This work was also supported by the Czech Science Foundation (P208/12/G016) and the operational program Research and Development for Innovations of the European Social Fund (CZ 1.05/2.1.00/03/0058).

REFERENCES

(1) Barbosa, A. G. H.; Barcelos, A. M. The Electronic Structure of the F_2, Cl_2, Br_2 Molecules: The Description of Charge-Shift Bonding within the Generalized Valence Bond Ansatz. *Theor. Chem. Acc.* **2009**, *122*, 51−66.

(2) Munusamy, E.; Sedlak, R.; Hobza, P. On The Nature of the Stabilization of Benzene···Dihalogen and Benzene···Dinitrogen Complexes: CCSD(T)/CBS and DFT-SAPT Calculations. *ChemPhysChem* **2011**, *12*, 3253−3261.

(3) Politzer, P.; Murray, J. S.; Clark, T. Halogen Bonding: An Electrostatically Driven Highly Directional Noncovalent Interaction. *Phys. Chem. Chem. Phys.* **2010**, *12*, 7748−7757.
(4) Clark, T.; Hennemann, M.; Murray, J. S.; Politzer, P. Halogen Bonding: The σ-Hole. *J. Mol. Model.* **2007**, *13*, 291−296.
(5) Politzer, P.; Lane, P.; Concha, M. C.; Ma, Y.; Murray, J. S. An Overview of Halogen Bonding. *J. Mol. Model.* **2007**, *13*, 305−311.
(6) Desiraju, G. R.; Shing Ho, P.; Kloo, L.; Legon, A. C.; Marquardt, R.; Metrangolo, P.; Politzer, P.; Resnati, G.; Rissanen, K. Definition of the Halogen Bond. *Pure Appl. Chem.* **2013**, *85*, 1711−1713.
(7) Muller, P. Glossary of Terms Used in Physical Organic Chemistry. *Pure Appl. Chem.* **1994**, *66*, 1077−1184.
(8) Duarte, D. J. R.; Angelina, E. L.; Peruchena, N. M. On the Strength of the Halogen Bonds: Mutual Penetration, Atomic Quadrupole Moment and Laplacian Distribution of the Charge Density Analysis. *Comput. Theor. Chem.* **2012**, *998*, 164−172.
(9) Politzer, P.; Laurence, P. R.; Jayasuriya, K. Molecular Electrostatic Potentials: An Effective Tool for the Elucidation of Biochemical Phenomena. *Environ. Health Perspect.* **1985**, *61*, 191−202.
(10) Murray, J. S.; Politzer, P. Statistical Analysis of the Molecular Surface Electrostatic Potential: An Approach to Describing Noncovalent Interactions in Condensed Phases. *J. Mol. Struct.: THEOCHEM* **1998**, *425*, 107−114.
(11) Politzer, P.; Murray, J. S. Representation of Condensed Phase Properties in Terms of Molecular Surface Electrostatic Potentials. *Trends Chem. Phys.* **1999**, *7*, 157−168.
(12) Politzer, P.; Murray, J. S.; Peralta-Inga, Z. Molecular Surface Electrostatic Potentials in Relation to Noncovalent Interactions in Biological Systems. *Int. J. Quantum Chem.* **2001**, *85*, 676−684.
(13) Becke, A. D. Density-Functional Thermochemistry. V. Systematic Optimization of Exchange-correlation Functionals. *J. Chem. Phys.* **1997**, *107*, 8554−8560.
(14) Schmider, H. L.; Becke, A. D. Optimized Density Functionals from the Extended G2 Test Set. *J. Chem. Phys.* **1998**, *108*, 9624−9631.
(15) Hartree, D. R. The Wave Mechanics of an Atom with a Non-Coulomb Central Field. Part I. Theory and Methods. *Math. Proc. Cambridge Philos. Soc.* **1928**, *24*, 89−110. Fock, V. Näherungsmethode zur Lösung des quantenmechanischen Mehrkörperproblems. *Z. Phys.* **1930**, *61*, 126−148.
(16) Dunning, T. H., Jr. Gaussian Basis Sets for Use in Correlated Molecular Calculations. I. The Atoms Boron Through Neon and Hydrogen. *J. Chem. Phys.* **1989**, *90*, 1007−1023.
(17) Davidson, E. R. Comment on Comment on Dunning's Correlation-Consistent Basis Sets. *Chem. Phys. Lett.* **1996**, *260*, 514−518.
(18) Kendall, R. A.; Dunning, T. H., Jr.; Harrison, R. J. Electron Affinities of the First-Row Atoms Revisited. Systematic Basis Sets and Wave Functions. *J. Chem. Phys.* **1992**, *96*, 6796−6806.
(19) Woon, D. E.; Dunning, T. H., Jr. Gaussian-Basis Sets for Use in Correlated Molecular Calculations. 3. The Atoms Aluminum Through Argon. *J. Chem. Phys.* **1993**, *98*, 1358−1371.
(20) Perdew, J. P.; Burke, K.; Ernzerhof, M. Generalized Gradient Approximation Made Simple. *Phys. Rev. Lett.* **1996**, *77*, 3865−68.
(21) Perdew, J. P.; Burke, K.; Ernzerhof, M. Errata: Generalized Gradient Approximation Made Simple. *Phys. Rev. Lett.* **1997**, *78*, 1396.
(22) Adamo, C.; Barone, V. Toward Reliable Density Functional Methods without Adjustable Parameters: The PBE0 Model. *J. Chem. Phys.* **1999**, *110*, 6158−6169.
(23) Møller, C.; Plesset, M. S. Note on an Approximation Treatment for Many-Electron Systems. *Phys. Rev.* **1934**, *46*, 618−622.
(24) Pople, J. A.; Seeger, R.; Krishnan, R. Variational Configuration Interaction Methods and Comparison with Perturbation Theory. *Int. J. Quantum Chem.* **1977**, *12* (Suppl. S11), 149−163.
(25) Bader, R. F. W.; Carroll, M. T.; Cheeseman, J. R.; Chang, C. Properties of Atoms in Molecules: Atomic Volumes. *J. Am. Chem. Soc.* **1987**, *109*, 7968−7979.
(26) Kolář, M.; Hostaš, J.; Hobza, P. The Strength and Directonality of the Halogen Bond Are Co-Determined by the Magnitude and Size of the σ-Hole. *Phys. Chem. Chem. Phys.* **2014**, *16*, 9987−9996.
(27) Pitonak, M.; Riley, K. E.; Neogrady, P.; Hobza, P. Highly Accurate CCSD(T) and DFT−SAPT Stabilization Energies of H-Bonded and Stacked Structures of the Uracil Dimer. *ChemPhysChem* **2008**, *9*, 1636−1644.
(28) Zierkiewicz, W.; Michalska, D.; Hobza, P. Adenine Ribbon Stabilized by Watson−Crick and Hoogsteen Hydrogen Bonds: WFT and DFT Study. *Phys. Chem. Chem. Phys.* **2010**, *12*, 2888−2894.
(29) Rezac, J.; Hobza, P. Extrapolation and Scaling of the DFT-SAPT Interaction Energies toward the Basis Set Limit. *J. Chem. Theory Comput.* **2011**, *7*, 685−689.
(30) Ran, J.; Hobza, P. Nature of Bonding in Nine Planar Hydrogen-Bonded Adenine···Thymine Base Pairs. *J. Phys. Chem. B* **2009**, *113*, 2933−2936.
(31) Riley, K. E.; Pitonak, M.; Cerny, J.; Hobza, P. On the Structure and Geometry of Biomolecular Binding Motifs (Hydrogen-bonding, Stacking, X−H···π): WFT and DFT Calculations. *J. Chem. Theory Comput.* **2010**, *6*, 66−80.
(32) Riley, K. E.; Hobza, P. Noncovalent Interactions in Biochemistry. *Wiley Interdiscip. Rev.: Comput. Mol. Sci.* **2011**, *1*, 3−17.
(33) Sponer, J.; Riley, K. E.; Hobza, P. Nature and Magnitude of Aromatic Stacking of Nucleic Acid Bases. *Phys. Chem. Chem. Phys.* **2008**, *10*, 2595−2610.
(34) Sedlak, R.; Jurecka, P.; Hobza, P. Density Functional Theory-Symmetry Adapted Perturbation Treatment Energy Decomposition of Nucleic Acid Base Pairs Taken from DNA Crystal Geometry. *J. Chem. Phys.* **2007**, *127*, 075104−075106.
(35) Hesselmann, A.; Korona, T. On the Accuracy of DFT-SAPT, MP2, SCS-MP2, MP2C, and DFT+Disp Methods for the Interaction Energies of Endohedral Complexes of the C_{60} Fullerene with a Rare Gas Atom. *Phys. Chem. Chem. Phys.* **2011**, *13*, 732−743.
(36) Karthikeyan, S.; Sedlak, R.; Hobza, P. On the Nature of Stabilization in Weak, Medium, and Strong Charge-Transfer Complexes: CCSD(T)/CBS and SAPT Calculations. *J. Phys. Chem. A* **2011**, *115*, 9422−9428.
(37) Sedlak, R.; Hobza, P.; Patwari, G. N. Hydrogen-Bonded Complexes of Phenylacetylene with Water, Methanol, Ammonia, and Methylamine. The Origin of Methyl Group-Induced Hydrogen Bond Switching. *J. Phys. Chem. A* **2009**, *113*, 6620−6625.
(38) Munusamy, E.; Sedlak, R.; Hobza, P. On the Nature of the Stabilization of Benzene···Dihalogen and Benzene···Dinitrogen Complexes: CCSD(T)/CBS and DFT-SAPT Calculations. *ChemPhysChem* **2011**, *12*, 3253−3261.
(39) Peterson, K. A.; Figgen, D.; Goll, E.; Stoll, H.; Dolg, M. Systematically Convergent Basis Sets with Relativistic Pseudopotentials. II. Small-core Pseudopotentials and Correlation Consistent Basis Sets for the Post-*d* Group 16−18 Elements. *J. Chem. Phys.* **2003**, *119*, 11113−11123.
(40) Peterson, K. A. Systematically Convergent Basis Sets With Relativistic Pseudopotentials. I. Correlation Consistent Basis Sets for the Post-*d* Group 13−15 Elements. *J. Chem. Phys.* **2003**, *119*, 11099−11112.
(41) Halkier, A.; Helgaker, T.; Jorgensen, P.; Klopper, W.; Olsen, J. Basis-set Convergence of the Energy in Molecular Hartree−Fock Calculations. *Chem. Phys. Lett.* **1999**, *302*, 437−446.
(42) Halkier, A.; Helgaker, T.; Jorgensen, P.; Klopper, W.; Koch, H.; Olsen, J.; Wilson, A. K. Basis-set Convergence in Correlated Calculations on Ne, N_2, and H_2O. *Chem. Phys. Lett.* **1998**, *286*, 243−252.
(43) Jurecka, P.; Sponer, J.; Cerny, J.; Hobza, P. Benchmark Database of Accurate (MP2 and CCSD(T) Complete Basis Set Limit) Interaction Energies of Small Model Complexes, DNA Base Pairs, and Amino Acid Pairs. *Phys. Chem. Chem. Phys.* **2006**, *8*, 1985−1993.
(44) Hobza, P.; Sponer, J. Toward True DNA Base-Stacking Energies: MP2, CCSD(T), and Complete Basis Set Calculations. *J. Am. Chem. Soc.* **2002**, *124*, 11802−11808.
(45) Jurecka, P.; Hobza, P. On the Convergence of the (Delta-E CCSD(T)-Delta-E-MP2) Term for Complexes with Multiple H-bonds. *Chem. Phys. Lett.* **2002**, *365*, 89−94.

(46) Dabkowska, I.; Jurecka, P.; Hobza, P. On Geometries of Stacked and H-bonded Nucleic Acid Base Pairs Determined at Various DFT, MP2 and CCSD(T) Levels up to the CCSD(T)/Complete Basis Set Limit Level. *J. Chem. Phys.* **2005**, *122*, 204322−204329.
(47) Zhao, Y.; Truhlar, D. G. The M06 Suite of Density Functionals for Main Group Thermochemistry, Thermochemical Kinetics, Noncovalent Interactions, Excited States, and Transition Elements: Two New Functionals and Systematic Testing of Four M06-class Functionals and 12 Other Functionals. *Theor. Chem. Acc.* **2008**, *120*, 215−241.
(48) Kozuch, S.; Martin, J. M. L. Halogen Bonds: Benchmarks and Theoretical Analysis. *J. Chem. Theory Comput.* **2013**, *9*, 1918−1931.
(49) Grimme, S.; Antony, J.; Ehrlich, S.; Krieg, H. A Consistent and Accurate ab initio Parametrization of Density Functional Dispersion Correction (DFT-D) for the 94 Elements H-Pu. *J. Chem. Phys.* **2010**, *132*, 154104−154123.
(50) Grimme, S.; Ehrlich, S.; Goerigk, L. Effect of the Damping Function in Dispersion Corrected Density Functional Theory. *J. Comput. Chem.* **2011**, *32*, 1456−1465.
(51) Jeziorski, B.; Moszynski, R.; Szalewicz, K. Perturbation Theory Approach to Intermolecular Potential Energy Surfaces of van der Waals Complexes. *Chem. Rev.* **1994**, *94*, 1887−1930.
(52) Grüning, M.; Gritsenko, O. V.; van Gisbergen, S. J. A.; Baerends, E. J. Shape Corrections to Exchange-Correlation Potentials by Gradient-Regulated Seamless Connection of Model Potentials for Inner and Outer Region. *J. Chem. Phys.* **2001**, *114*, 652−660.
(53) Hesselmann, A.; Jansen, G. First-order Intermolecular Interaction Energies from Kohn−Sham Orbitals. *Chem. Phys. Lett.* **2002**, *357*, 464−470.
(54) Hesselmann, A.; Jansen, G. Intermolecular Induction and Exchange-induction Energies from Coupled-perturbed Kohn−Sham Density Functional Theory. *Chem. Phys. Lett.* **2002**, *362*, 319−325.
(55) Hesselmann, A.; Jansen, G. Intermolecular Dispersion Energies from Time-dependent Density Functional Theory. *Chem. Phys. Lett.* **2003**, *367*, 778−784.
(56) Hesselmann, A.; Jansen, G. The Helium Dimer Potential from a Combined Density Functional Theory and Symmetry-adapted Perturbation Theory Approach Using an Exact Exchange−Correlation Potential. *Phys. Chem. Chem. Phys.* **2003**, *5*, 5010−5014.
(57) Hesselmann, A.; Jansen, G.; Schütz, M. Density-Functional Theory-Symmetry-Adapted Intermolecular Perturbation Theory with Density Fitting: A New Efficient Method to Study Intermolecular Interaction Energies. *J. Chem. Phys.* **2005**, *122*, 014103−014119.
(58) Jansen, G.; Hesselmann, A. Comment on: Using Kohn−Sham Orbitals in Symmetry-Adapted Perturbation Theory to Investigate Intermolecular Interactions. *J. Phys. Chem. A* **2001**, *105*, 11156−11157.
(59) Misquitta, A. J.; Szalewicz, K. Intermolecular Forces from Asymptotically Corrected Density Functional Description of Monomers. *Chem. Phys. Lett.* **2002**, *357*, 301−306.
(60) Stone, A. J. Distributed Multipole Analysis, or How to Describe a Molecular Charge Distribution. *Chem. Phys. Lett.* **1981**, *83*, 233−239.
(61) Stone, A. J.; Alderton, M. Distributed Multipole Analysis Methods and Applications. *Mol. Phys.* **1985**, *56*, 1047−1064.
(62) Stone, A. J. Distributed Multipole Analysis: Stability for Large Basis Sets. *J. Chem. Theory Comput.* **2005**, *1*, 1128−1132.
(63) Stone, A. J. *GDMA: Distributed Multipoles from Gaussian 98 Wavefunctions*, version 2.2.04; Tech. Rep., University of Cambridge, 1998.
(64) Stone, A. J.; Dullweber, A.; Engkvist, O.; Fraschini, E.; Hodges, M. P.; Meredith, A. W.; Nutt, D. R.; Popelier, P. L. A.; Wales, D. J. *Orient: A Program for Studying Interactions Between Molecules*, version 4.6.16; University of Cambridge, Cabmridge, U.K., 2002; Enquiries to Stone, A. J. ajs1@cam.ac.uk.
(65) Werner, H.-J.; Knowles, P. J.; Manby, F. R.; Schütz, M.; Celani, P.; Knizia, G.; Korona, T.; Lindh, R.; Mitrushenkov, A.; Rauhut, G.; et al. *MOLPRO, A Package of ab initio Programs*, version 2010.1; 2010; http://www.molpro.net.
(66) TURBOMOLE V6.3 2011, A Development of the University of Karlsruhe and the Forschungszentrum Karlsruhe GmbH, 1989−2007; TURBOMOLE GmbH, since 2007; available from http://www.turbomole.com.
(67) Reed, A. E.; Curtiss, L. A.; Weinhold, F. Intermolecular Interactions from a Natural Bond Orbital, Donor-Acceptor Viewpoint. *Chem. Rev.* **1988**, *88*, 899−926.
(68) Frisch, M. J.; Trucks, G. W.; Schlegel, H. B.; Scuseria, G. E.; Robb, M. A.; Cheeseman, J. R.; Scalmani, G.; Barone, V.; Mennucci, B.; Petersson, G. A.; et al. *Gaussian 09*, Revision D.01; Gaussian, Inc.: Wallingford, CT, 2009.
(69) Boys, S. F.; Bernardi, F. The Calculation of Small Molecular Interactions by the Differences of Separate Total Energies. Some Procedures with Reduced Errors. *Mol. Phys.* **1970**, *19*, 553−566.